1470 *Inorg. Chem.* **2011**, *50*, 1470–1479
DOI: 10.1021/ic102044z

Inorganic Chemistry
Article

Synthesis and Reactivity of *o*-Benzylphosphino- and *o*-α-Methylbenzyl(*N,N*-dimethyl)amine-Boranes

Zachariah M. Heiden, Michael Schedler, and Douglas W. Stephan*

Department of Chemistry, University of Toronto, 80 St. George St., Toronto, Ontario M5S 3H6, Canada

Received October 8, 2010

The series of *o*-benzylphosphino-boranes, *o*-(R_2B)$C_6H_4CH_2PtBu_2$ (R = Cl **3**, Ph **4**, Cy **6**, C_6F_5 **7**, Mes **8**) and *o*-(BBN)$C_6H_4CH_2PtBu_2$ (**5**), were synthesized from reactions of the respective chloroboranes with the lithiated benzylphosphine. In an analogous fashion, the α-methylbenzyl(*N,N*-dimethyl)amine-boranes *o*-(R_2B)$C_6H_4CH(Me)NMe_2$ (R = Cl **10**, Ph **11**, Cy **12**, C_6F_5 **13**, Mes **14**) were prepared. While these species were inactive in the catalytic hydrogenation of *t*BuN=CHPh, compounds **7**, **8**, and **14** did react with H_2 at elevated temperatures (100 °C), resulting in the elimination of HC_6F_5 and mesitylene, respectively. In the latter case, the species *o*-((Mes)HB)$C_6H_4CH(Me)NMe_2$ **15** was isolated. **14** was also shown to react with H_2O to give the species *o*-((Mes)(HO)B)$C_6H_4CH(Me)NMe_2$ **16** with the loss of mesitylene. The structure of these compounds and the nature of these reactions were also probed spectroscopically, crystallographically, and computationally. The energies for the products of hydrogenation, the phosphonium and ammonium hydridoborates, were computed. In all cases, these products were endothermic with respect to the precursor phosphine-boranes and amine-boranes and H_2. The barriers to H_2 activation were found to be in the range of 24−38 kcal/mol. These theoretical studies also demonstrate that the steric bulk around the boron center dramatically affects the activation barrier for H_2 activation, while the Lewis acidity of the borane has the largest effect on the stabilization of the resulting onium-borohydride. In the case of the elimination reactions, the driving forces appear to be the loss of arene byproduct and formation of a strong donor−acceptor bond.

Introduction

The use of hydrogenation catalysis is critical to the production of a large range of chemicals, materials, and products, including upgraded crude oil, production of bulk commodity materials, and the preparation of food, agricultural, and pharmaceutical products. In addition, hydrogenation is an important process in synthetic organic chemistry. While homogeneous or heterogeneous transition metal-based catalysts are currently used in these processes, recent research efforts have targeted metal free reducing agents. While these efforts are interesting from a fundamental science perspective, they also offer ways to avoid the use of expensive transition metal catalysts[1] and their removal from the reaction products. The latter issue is generally a major concern for the pharmaceutical industry where toxicity concerns are of paramount importance.[2,3] Known main-group reducing reagents are typically stoichiometric reductions, and result in tedious procedures and toxic chemical waste.[4,5]

In 2006, we demonstrated the first nonmetal system that reversibly activates H_2.[6] This species which was an arene-linked phosphine/borane species (Chart 1, A) was also shown to be a metal-free catalyst for the hydrogenation of sterically bulky imines.[6−10] This development was based on the concept of "frustrated" Lewis pairs (FLPs). Subsequently Erker and co-workers applied the species $Mes_2PC_2H_4B(C_6F_5)_2$ (Chart 1, B) complex,[11,12] in the catalytic hydrogenation of imines, enamines, and silyl enol ethers. Rieger et al developed a related N/B catalyst based on a linked tetramethylpiperidine and a borane center (Chart 1, C).[13,14] In an effort to

*To whom correspondence should be addressed. E-mail: dstephan@chem.utoronto.ca.

(1) Enthaler, S.; Junge, K.; Beller, M. *Angew. Chem., Int. Ed.* **2008**, *47*, 3317–3321.
(2) Garrett, C. E.; Prasad, K. *Adv. Synth. Catal.* **2004**, *346*, 889–900.
(3) Elemental Impurities - Limits. In *Pharmacopeial Forum*; U.S. Pharmacopeia: Rockville, MD, 2010; Vol. *36*, p 1.
(4) Yaragorla, S. *Synlett* **2008**, 3073–3074.
(5) Zhenjiang, L. *Synlett* **2005**, 182–183.
(6) Welch, G. C.; San Juan, R. R.; Masuda, J. D.; Stephan, D. W. *Science* **2006**, *314*, 1124–1126.
(7) Chase, P. A.; Welch, G. C.; Jurca, T.; Stephan, D. W. *Angew. Chem., Int. Ed.* **2007**, *46*, 8050–8053.
(8) Chase, P. A.; Jurca, T.; Stephan, D. W. *Chem. Commun.* **2008**, 1701–1703.
(9) Stephan, D. W.; Erker, G. *Angew. Chem., Int. Ed.* **2010**, *49*, 46–76.
(10) Chen, D.; Klankermayer, J. *Chem. Commun.* **2008**, 2130–2131.
(11) Spies, P.; Erker, G.; Kehr, G.; Bergander, K.; Froehlich, R.; Grimme, S.; Stephan, D. W. *Chem. Commun.* **2007**, 5072–5074.
(12) Spies, P.; Schwendemann, S.; Lange, S.; Kehr, G.; Froehlich, R.; Erker, G. *Angew. Chem., Int. Ed.* **2008**, *47*, 7543–7546.
(13) Sumerin, V.; Schulz, F.; Atsumi, M.; Wang, C.; Nieger, M.; Leskelae, M.; Repo, T.; Pyykkoe, P.; Rieger, B. *J. Am. Chem. Soc.* **2008**, *130*, 14117–14119.
(14) Sumerin, V.; Schulz, F.; Nieger, M.; Atsumi, M.; Wang, C.; Leskelae, M.; Pyykkoe, P.; Repo, T.; Rieger, B. *J. Organomet. Chem.* **2009**, *694*, 2654–2660.

 Published on Web 01/26/2011

Chart 1. Metal-Free Bifunctional Hydrogenation Catalysts

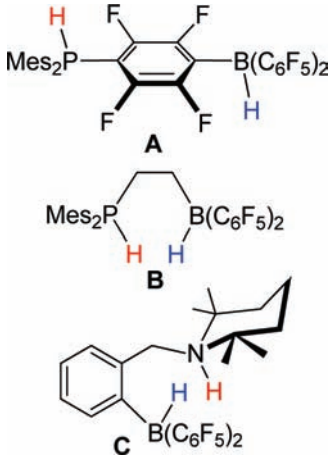

explore related bifunctional systems, herein, we report the synthesis of a series of phosphine-borane and amine-borane species in which a benzylic fragment links the Lewis acid and donor sites. The impact of the nature of the donor as well as variation of the substituents on B is examined. Reactions with H_2 are probed and the relationship between structure and reactivity is probed experimentally and computationally. The ramifications for the design of new bifunctional hydrogenation catalysts are discussed.

Experimental Section

Materials and Methods. All preparations and manipulations were performed on a double manifold N_2/vacuum line with Schlenk-type glassware or in a N_2-filled VAC glovebox. Solvents were dried using an Innovative Technologies solvent system, and degassed before use. NMR spectra were obtained on a Bruker Avance 400 MHz spectrometer, and spectra were referenced to residual solvent (^{1}H, ^{13}C) or externally (^{11}B; $BF_3 \cdot OEt_2$, ^{19}F; $CFCl_3$, ^{31}P; 85% H_3PO_4). Chemical shifts are reported in parts per million (ppm). NMR solvents were purchased from Cambridge Isotopes, dried over CaH_2 or Na/benzophenone, vacuum distilled prior to use and stored over 4 Å molecular sieves in the glovebox. $B(C_6F_5)_3$ was generously provided by Nova Chemicals (from Boulder Scientific Company). $ClB(C_6F_5)_2$ was prepared according to the literature procedure previously reported by Piers and co-workers.[15] Combustion analysis was performed in house on a Perkin-Elmer CHN Analyzer. (±)-α-methylbenzylamine was purchased from Aldrich and used as received. *o*-$LiC_6H_4CH(Me)NMe_2$ (**9**) was prepared according the procedure previously reported by Payne and Stephan.[16]

Synthesis of *o*-$BrC_6H_4CH_2PtBu_2$ (1). The known compound, **1**,[17] was prepared by a similar route that was used to prepare $C_6H_5CH_2PtBu_2$.[18,19] $HPtBu_2$ (4.42 g, 30.23 mmol) was dissolved in degassed acetone and a solution of *o*-$BrC_6H_4CH_2Br$ (7.56 g, 30.23 mmol) in 75 mL of degassed acetone was added. After 30 min of refluxing a white precipitate started to form. The mixture was refluxed for 16 h, cooled to room temperature, and 100 mL of dry pentane was added to complete the precipitation. The solid was separated via filtration and dissolved in 100 mL of degassed water. The solution was added to a solution of sodium acetate (25 g) in degassed water (100 mL). The aqueous phase was anaerobically extracted with ether. The mixed ether phases were dried with $MgSO_4$, and the ether removed under vacuum. Distillation of the residue gave **1** (4.91 g, 15.6 mmol; 52%) as a colorless oil. ^{1}H NMR (C_6D_6) 1.08 (d, $^3J_{PH}$ = 10.9 Hz, 18 H, *t*Bu), 2.97 (d, $^2J_{PH}$ = 3.2 Hz, 2 H, CH_2), 6.65 (td, $^3J_{HH}$ = 8.0 Hz, $^5J_{HH}$ = 1.9, 1 H, Ph), 6.96 (td, $^3J_{HH}$ = 7.7 Hz, $^5J_{HH}$ = 1.4 Hz, 1 H, Ph.), 7.41 (dd, $^3J_{HH}$ = 8.3 Hz, $^5J_{HH}$ = 1.5 Hz, 1 H, Ph), 7.79 (m, 1 H, Ph); ^{31}P NMR (C_6D_6) 34.2 (br). Anal. Calcd for $C_{15}H_{24}BrP$: C: 57.15%, H: 7.67%; Found: C: 57.59%, H: 7.95%.

Generation of $LiC_6H_4CH_2PtBu_2$ (2). This procedure is a slight variation of the reported method.[17] **1** (1.60 g, 5.09 mmol) was dissolved in hexanes (30 mL) and *n*BuLi in hexanes (2.45 mL, 6.10 mmol, 2.5 M) was added via syringe, resulting in the immediate formation of a white precipitate. The mixture was stirred 1 h at room temperature. The mixture was filtered in a glovebox and **2** (1.20 g, 4.94 mmol; 97%) was obtained as a white solid. The product was used without further purification. **2**: ^{1}H NMR (C_6D_6) 1.03 (d, $^3J_{PH}$ = 11.0 Hz, 18 H, *t*Bu), 3.20 (d, $^2J_{PH}$ = 4.4 Hz, 2 H, CH_2), 7.03−7.17 (m, 3 H, Ph), 8.11 (d, $^3J_{HH}$ = 6.5 Hz, 1 H, Ph); ^{31}P NMR (C_6D_6) 32.5 (br s).

Synthesis of *o*-$(Cl_2B)C_6H_4CH_2PtBu_2$ (3). Compound **2** (120 mg, 0.50 mmol) was dissolved in toluene (20 mL) and BCl_3 in hexanes (0.5 mL, 0.5 mmol, 1.0 M) was added with a syringe. An initially purple solution became a colorless solution containing a slightly yellow solid after stirring the solution for 4 days. The mixture was filtered, and the solvent of the filtrate was removed under reduced pressure resulting in a slightly yellow solid. The solid was recrystallized from a toluene/hexanes mixture to give a colorless solid (60 mg, 0.18 mmol, 38%). ^{1}H NMR (C_7D_8): 1.08 (d, $^3J_{PH}$ = 13.2 Hz, 18 H, *t*Bu), 2.72 (d, $^2J_{PH}$ = 9.4 Hz, 2 H, CH_2), 6.85 (d, $^3J_{HH}$ = 7.4 Hz, 1 H, Ph), 7.06 (td, $^3J_{HH}$ = 7.6 Hz, $^5J_{HH}$ = 1.4 Hz, 1 H, Ph), 7.14 (t, $^3J_{HH}$ = 7.5 Hz, 1 H, Ph), 7.92 (d, $^3J_{HH}$ = 7.3 Hz, 1 H, Ph); ^{11}B NMR (C_7D_8) 0.02 (d, $^1J_{BP}$ = 96.5 Hz); ^{31}P NMR (C_7D_8) 31.2 (br s). Anal. Calcd for $C_{15}H_{24}BCl_2P$: C: 56.83%, H: 7.63%; Found: C: 56.99%, H: 7.75%.

Synthesis of *o*-$(Ph_2B)C_6H_4CH_2PtBu_2$ (4). Method (i): This species was prepared via reaction of (**2**) and $ClBPh_2$ as described below for compounds **5**−**8**. Yield: 61%. Method (ii): **3** (45 mg, 0.14 mmol) was dissolved in 10 mL of toluene and PhLi (0.3 mL, 0.56 mmol, 1.8 M) in di-*n*-butylether was added with a syringe at room temperature. The mixture turned deep red because of the color of the phenyllithium solution. The mixture was stirred overnight and turned nearly colorless. Removal of the solvent gave a slightly yellow solid. Complete conversion was confirmed by NMR spectroscopy. ^{1}H NMR (C_7D_8) 0.76 (d, $^3J_{PH}$ = 12.0 Hz, 18 H, *t*Bu), 2.99 (d, $^2J_{PH}$ = 8.8 Hz, 2 H, CH_2), 7.13 (d, $^3J_{HH}$ = 7.1 Hz, 2 H, *p*-Ph), 7.17−7.21 (m, 3 H, Ph), 7.23 (t, $^3J_{HH}$ = 7.3 Hz, 4 H, *p*-Ph), 7.70 (br, 1 H, Ph), 7.79 (d, J_{HH} = 7.4 Hz, 4 H, *o*-Ph); ^{11}BNMR (C_7D_8) −0.5 (br s); ^{31}P NMR (C_7D_8) 38.2 (br s). Anal. Calcd for $C_{27}H_{34}BP$: C: 81.00%, H: 8.56%; Found: C: 81.05%, H: 8.77%.

Synthesis of *o*-$(BBN)C_6H_4CH_2PtBu_2$ (5), *o*-$(R_2B)C_6H_4CH_2PtBu_2$ (R = Cy 6, C_6F_5 7, Mes 8). These compounds were prepared in a similar fashion using the corresponding boron-chloride precursor and thus only one preparation is detailed. **2** (182 mg, 0.75 mmol) was dissolved in toluene (40 mL) and Cy_2BCl (0.75 mL, 0.75 mmol, 1.0 M) in hexanes was added with a syringe. After 30 min the colorless solution became milky. After 18 h of stirring at room temperature the mixture of a colorless solution and a slightly yellow precipitate was filtered, and the solvent of the filtrate was removed under reduced pressure. The resulting colorless oil was dissolved in hexanes and stirred for 1 h. Removal of the hexanes gave 246 mg (0.60 mmol, 80%) of **6**, a colorless solid.

5: yield 140 mg, 0.37 mmol, 90%. ^{1}H NMR (C_7D_8) 0.98 (d, $^3J_{PH}$ = 11.2 Hz, 18 H, tBu), 1.36−2.39 (br, 14 H, BBN), 2.8

(15) Parks, D. J.; Piers, W. E.; Yap, G. P. A. *Organometallics* **1998**, *17*, 5492–5503.
(16) Payne, N. C.; Stephan, D. W. *Inorg. Chem.* **1982**, *21*, 182–188.
(17) Abicht, H. P.; Issleib, K. *J. Organomet. Chem.* **1980**, *185*, 265–75.
(18) Abicht, H. P.; Baumeister, U.; Hartung, H.; Issleib, K.; Jacobson, R. A.; Richardson, J.; Socol, S. M.; Verkade, J. G. *Z. Anorg. Allg. Chem.* **1982**, *494*, 55–66.
(19) Abicht, H. P. *J. Organomet. Chem.* **1986**, *311*, 57–61.

(d, $^2J_{PH}$ = 7.5 Hz, 2 H, CH_2), 6.99 (d, $^3J_{HH}$ = 6.0 Hz, 1 H, Ph), 7.10 (t, $^3J_{HH}$ = 4.0 Hz, 1 H, Ph), 7.19 (t, $^3J_{HH}$ = 7.5 Hz, 1 H, Ph), 7.95 (d, $^3J_{HH}$ = 7.7 Hz, 1 H, Ph); ^{11}B NMR (C_7D_8) 7.2 (br s); ^{31}P NMR (C_7D_8) 42.2 (br s) Anal. Calcd for $C_{23}H_{38}BP$: C 77.53%, H 10.75%; Found: C 77.56%, H 10.46%.

6: yield 246 mg, 0.60 mmol, 80%. ^{1}H NMR (C_7D_8) 0.99 (d, $^3J_{PH}$ = 10.8 Hz, 18 H, tBu), 1.2−2.1 (m, Cy), 2.84 (d, $^2J_{PH}$ = 6.4 Hz, 2 H, CH_2), 6.99 (d, $^3J_{HH}$ = 5.7 Hz, 1 H, Ph), 7.07 (td, $^3J_{HH}$ = 7.4 Hz, $^5J_{HH}$ = 1.4 Hz, 1 H, Ph), 7.15 (t, $^3J_{HH}$ = 7.0 Hz, 1 H, Ph), 7.57 (d, $^3J_{HH}$ = 7.6 Hz, 1 H, Ph); ^{11}B NMR (C_7D_8) 13.5 (br s); ^{31}P NMR (C_7D_8) 47.1 (br s). Anal. Calcd for $C_{27}H_{40}BP$: C: 79.80%, H: 9.92%; Found: C: 79.43%, H: 9.95%.

7: yield 120 mg, 0.21 mmol, 61%. ^{1}H NMR (C_7D_8) 0.75 (d, $^3J_{PH}$ = 12.4 Hz, 18 H, *t*Bu), 2.87 (br, 2 H, CH_2), 6.94−7.11 (m, 3 H, Ph), 7.45 (br, 1 H, Ph); ^{11}B NMR (C_7D_8) −7.79 (br s); ^{19}F NMR (C_7D_8) −163.4 (br, 2F, F_m), −157.1 (s, br., 1 F, F_p), −127.5 (br, 2 F, F_o); ^{31}P NMR (C_7D_8) 53.2 (br). Anal. Calcd for $C_{27}H_{24}F_{10}BP$: C: 55.89%, H: 4.17%; Found: C: 56.40%, H: 4.46%.

8: yield 192 mg, 0.39 mmol, 72%. yellow solid. ^{1}H NMR (C_7D_8) 0.97 (br s, 18 H, tBu), 2.1−2.35 (br s, 18 H, Mes-CH_3), 2.89 (br s, 2 H, CH_2), 6.71 (br s, 2 H, Mes-H), 6.96 (d, $^3J_{HH}$ = 7.2 Hz, 1 H, Ph), 7.21 (td, $^3J_{HH}$ = 7.4 Hz, $^5J_{HH}$ = 1.5 Hz, 1 H, Ph), 7.41 (d, $^3J_{HH}$ = 7.4 Hz, 1 H, Ph), 8.11 (dd, $^3J_{HH}$ = 7.9 Hz, $^5J_{HH}$ = 4.8 Hz, 1 H, Ph); ^{11}B NMR (C_7D_8) 37 (v br, s); ^{31}P NMR (C_7D_8) 23.9 (br s) Anal. Calcd for $C_{33}H_{46}BP$: C: 81.81%, H: 9.57%; Found: C: 81.43%, H: 9.67%.

Synthesis of (±) *o*-(R_2B)C_6H_4CH(Me)NMe_2 (R = Cl 10, Ph 11, Cy 12, C_6F_5 13, Mes 14). These compounds were prepared in a similar fashion using the corresponding boron-chloride precursor and thus only one preparation is detailed. A 0.6 mL portion (0.6 mmol) of a 1.0 M BCl_3 in hexanes solution was added to a slurry of 0.10 g (0.6 mmol) of complex **9** in 15 mL of toluene, precooled to −78 °C, resulting in an immediate color change from a gray colored slurry to a white colored slurry. The solution was allowed to warm to room temperature, and the white precipitate was removed by filtration. The solvent was removed of the resulting colorless filtrate under reduced pressure. The colorless solid was recrystallized from diethyl ether.

10: yield 185 mg (80%). ^{1}H NMR ($CDCl_3$) 1.55 (d, $^3J_{HH}$ = 6.7 Hz, 3H, NCH*Me*), 2.41 (s, 3H, *Me*MeNC), 2.88 (s, 3H, Me-*Me*NC), 4.60 (q, $^3J_{HH}$ = 6.7 Hz, 1H, NC*H*Me), 7.02 (d, $^3J_{HH}$ = 7.2 Hz, 1H, Ph), 7.20−7.32 (m, 2H, Ph), 7.54 (d, $^3J_{HH}$ = 6.9 Hz, 1H, Ph). ^{11}B NMR ($CDCl_3$) 9.3 (s). Anal. Calcd for $C_{10}H_{14}BCl_2N$: C: 52.39%; H: 6.16%; N: 6.11%. Found: C: 52.68%; H: 6.84%; N: 6.12%.

11: yield 160 mg (80%). ^{1}H NMR (C_6D_6): 0.68 (d, $^3J_{HH}$ = 6.8 Hz, 3H, NCH*Me*), 1.44 (s, 3H, *Me*MeNC), 1.96 (s, 3H, Me*Me*NC), 3.84 (q, $^3J_{HH}$ = 6.8 Hz, 1H, NC*H*Me), 6.89 (d, $^3J_{HH}$ = 7.1 Hz, 1H, $C_6H_4BPh_2$), 7.16−7.35 (m, 6H, Ph), 7.39 (t, $^3J_{HH}$ = 8.3 Hz, 2H, Ph), 7.59 (d, $^3J_{HH}$ = 8.3 Hz, 2H, Ph), 7.76 (d, $^3J_{HH}$ = 7.2 Hz, 1H, Ph), 8.01 (d, $^3J_{HH}$ = 8.3 Hz, 2H, Ph). ^{11}B NMR (C_6D_6) 6.7 (s). Anal. Calcd for $C_{22}H_{24}BN$: C: 84.29%, H: 7.72%, N: 4.47%; Found: C: 84.10%, H: 7.70%, N: 4.51%.

12: yield 210 mg (81%). ^{1}H NMR (C_6D_6) 0.74 (d, $^3J_{HH}$ = 7.7 Hz, 3H, NCH*Me*), 0.78−2.05 (m, 22H, Cy), 1.67 (s, 3H, *Me*MeNC), 1.98 (s, 3H, Me*Me*NC), 3.98 (q, $^3J_{HH}$ = 6.9 Hz, 1H, NC*H*Me), 6.81 (d, $^3J_{HH}$ = 8.0 Hz, 1H, Ph), 7.16 (m, 1H, Ph), 7.27 (tt, $^5J_{HH}$ = 1.1 $^3J_{HH}$ = 7.1 Hz, 1H, Ph), 7.53 (d, $^3J_{HH}$ = 7.3 Hz, 1H, Ph). ^{11}B NMR (C_6D_6) 8.7 (s). Anal. Calcd for $C_{22}H_{36}BN$: C: 81.16%; H: 11.15%; N: 4.30%. Found: C: 80.92%; H: 11.03%; N: 4.22%.

13: yield 178 mg (56%). ^{1}H NMR (C_6D_5Br) 1.19 (d, $^3J_{HH}$ = 6.6 Hz, 3H, NCH*Me*), 1.83 (s, 3H, *Me*MeNC), 2.57 (s, 3H, Me-*Me*NC), 4.81 (q, $^3J_{HH}$ = 6.6 Hz, 1H, NC*H*Me), 6.87 (d, $^3J_{HH}$ = 7.3 Hz, 1H, C_6H_4), 7.12 (t, $^3J_{HH}$ = 7.3 Hz, 1H, C_6H_4), 7.21 (t, $^3J_{HH}$ = 7.3 Hz, 1H, C_6H_4), 7.72 (br d, $^3J_{HH}$ = 7.3 Hz, 1H, C_6H_4). ^{11}B NMR (C_6D_5Br) 2.0 (s). ^{19}F NMR (C_6D_5Br) −125.4 (d, $^5J_{FF}$ = 7.2, 25.4 Hz, *o*-F), −126.6 (dd, $^5J_{FF}$ = 7.2 $^3J_{FF}$ = 25.4 Hz, *o*-F), −155.1 (t, $^3J_{FF}$ = 21.3 Hz, *p*-F), −158.1 (t, $^3J_{FF}$ = 21.3 Hz, *p*-F), −161.7 (m, *m*-F). Anal. Calcd for $C_{22}H_{14}BF_{10}N$: C: 53.54%; H: 2.86%; N: 2.84%. Found: C: 53.59%; H: 3.36%; N: 2.80%.

14: yield 167 mg (65%). ^{1}H NMR (C_7D_8) 0.96 (br s, 3H, Me_2NCH*Me*), 1.86 (br s, 6H, *Me*$_2$NCHMe), 1.86 (br s, 3H, $C_6Me_3H_2$, 2.04 (br s, 3H, $C_6Me_3H_2$, 2.12 (br s, 3H, $C_6Me_3H_2$, 2.19 (br s, 9H, $C_6Me_3H_2$, 3.95 (br s, 1H, Me_2NC*H*Me), 6.64 (br s, 1H, Ph), 6.73 (br s, 2H, Ph), 6.80 (br s, 1H, Ph), 7.02 (m, 2H, Ph), 7.15−7.30 (br m, 2H, Ph), 7.42 (br d, J = 8.2 Hz, 1H, Ph). ^{11}B NMR (C_6D_6) 73.9 (br s). Anal. Calcd for $C_{28}H_{36}BN$: C: 84.62%; H: 9.13%; N: 3.52%. Found: C: 84.55%; H: 9.03%; N: 3.44%.

Synthesis of (±) *o*-((Mes)HB)C_6H_4CH(Me)NMe_2 (15). A toluene solution of 100 mg (0.25 mmol) of **14** was pressurized with 1 H_2 at 77 K (~ 5 atm at 373 K), after degassing the solution through three freeze−pump−thaw cycles. The colorless solution was heated to 100 °C for 16 h. The solvent was removed under reduced pressure, and the formed mesitylene was removed by a hexane wash. The colorless solid was recrystallized from CH_2Cl_2 and hexanes. **15** was found to be air stable over the period of weeks. Yield: 60 mg (85%). ^{1}H NMR ($CDCl_3$) 1.53 (d, J = 7.2 Hz, 3H, minor-MeMeNCH*Me*), 1.55 (d, J = 7.3 Hz, 3H, major-MeMeNCH*Me*), 2.12 (d, J = 2.4 Hz, 6H, major-B(*Mes*)), 2.22 (s, 3H, minor-*Me*MeNC), 2.26 (s, 9H, minor-B(*Mes*)), 2.39 (s, 3H, minor-Me*Me*NC), 2.56 (s, 3H, major-B(*Mes*)), 2.60 (s, 3H, major-Me*Me*NC), 2.73 (s, 3H, major-*Me*MeNC), 4.18 (q, J = 7.0 Hz, 1H, major-MeMeNC*H*Me), 4.27 (q, J = 7.0 Hz, 1H, minor-MeMeNC*H*Me), 6.67−7.37 (12H, Ph). ^{11}B NMR ($CDCl_3$) 1.3 (br s). Anal. Calcd for $C_{19}H_{26}BN$: C: 81.73%; H: 9.39%; N: 5.02%. Found: C: 81.52%; H: 9.22%; N: 5.09%.

***o*-((Mes)HOB)C_6H_4CH(Me)NMe_2 (16). 16** was obtained as a decomposition product of **2** in moist air/wet solvents. ^{1}H NMR (C_6D_6) 1.36 (d, J = 6.9 Hz, 3H, Me_2NCH*Me*), 1.86 (s, 6H, $C_6Me_3H_2$), 2.30 (s, 3H, Me_2NCH*Me*), 2.45 (br s, 6H, *Me*$_2$N), 3.02 (q, J = 6.7 Hz, 1H, Me_2NC*H*Me), 6.92 (s, 2H, $C_6Me_3H_2$) 6.93−7.14 (m, 3H, Ph), 7.75 (d, J = 7.1 Hz, 1H, Ph), 13.87 (br s, 1H, BO*H*). ^{11}B NMR (C_6D_6) 47.6 (br s).

X-ray Data Collection and Reduction. Crystals were coated in Paratone-N oil in the glovebox, mounted on a MiTegen Micromount and placed under an N_2 stream, thus maintaining a dry, O_2-free environment for each crystal. The data were collected on a Bruker Apex II diffractometer. The data were collected at 150(±2) K for all crystals (Table 1). The frames were integrated with the Bruker SAINT software package using a narrow-frame algorithm. Data were corrected for absorption effects using the empirical multiscan method (SADABS).

Structure Solution and Refinement. Non-hydrogen atomic scattering factors were taken from the literature tabulations.[20] The heavy atom positions were determined using direct methods employing the SHELXTL direct methods routine. The remaining non-hydrogen atoms were located from successive difference Fourier map calculations. The refinements were carried out by using full-matrix least-squares techniques on F, minimizing the function $\omega (F_o - F_c)^2$ where the weight ω is defined as $4F_o^2/2\sigma(F_o^2)$ and F_o and F_c are the observed and calculated structure factor amplitudes, respectively. In the final cycles of each refinement, all non-hydrogen atoms were assigned anisotropic temperature factors in the absence of disorder or insufficient data. In the latter cases atoms were treated isotropically. C−H atom positions were calculated and allowed to ride on the carbon to which they are bonded assuming a C−H bond length of 0.95 Å. H-atom temperature factors were fixed at 1.10 times the isotropic temperature factor of the C-atom to which they are bonded. The H-atom contributions were calculated, but not refined. The locations of the largest peaks in the final difference

(20) Cromer, D. T.; Waber, J. T. *Int. Tables X-Ray Crystallogr.* **1974**, *4*, 71.

Table 1. Crystallographic Data

	3	**4**	**5**	**6**	**7**	**8**
formula	$C_{15}H_{24}BCl_2P$	$C_{27}H_{34}BP$	$C_{23}H_{38}BP$	$C_{27}H_{46}BP$	$C_{27}H_{24}BF_{10}P$	$C_{33}H_{46}BP$
formula weight	317.04	400.34	356.33	412.44	580.25	484.50
crystal system	orthorhombic	monoclinic	orthorhombic	monoclinic	triclinic	orthorhombic
space group	*Pbca*	*P*2(1)/*n*	*Pbca*	*P*2(1)/*c*	$P\bar{1}$	*P*2(1)2(1)2(1)
a (Å)	11.0177 (20)	11.6783 (9)	10.0869 (6)	8.7532(11)	9.4512 (4)	10.7842 (5)
b (Å)	12.8239 (21)	14.2236 (10)	16.8594 (10)	16.0435(21)	9.7356 (4)	15.3950 (6)
c (Å)	23.7562 (40)	14.0628 (9)	24.3705 (15)	17.5553(25)	14.8664 (6)	17.7979 (8)
α (deg)	90.00	90.00	90.00	90.00	104.5766 (25)	90.00
β (deg)	90.00	93.380 (3)	90.00	90.7844 (90)	90.3618 (21)	90.00
γ (deg)	90.00	90.00	90.00	90.00	99.9471 (22)	90.00
V (Å^3)	3356.52 (146)	2331.88 (46)	4144.404 (717)	2465.102(693)	1302.193 (111)	2954.871 (306)
Z	8	4	8	4	2	4
d(calc) g cm^{-1}	1.255	1.140	1.142	1.111	1.480	1.089
abs coeff, *μ*, cm^{-1}	4.7	1.3	1.4	1.2	1.9	1.1
data collected	3814	5701	4785	5664	7541	6969
data $F_o^2 > 3\sigma(F_o^2)$	2883	3872	3599	3463	3955	5102
variables	178	268	232	268	358	328
R	0.0353	0.0653	0.0387	0.1096	0.0492	0.0507
R_w	0.1228	0.2394	0.1085	0.3268	0.2162	0.1104
goodness of fit	0.839	0.754	0.957	1.119	0.779	1.014

	10	**11**	**12**	**13**	**15**	**16**
formula	$C_{10}H_{14}BCl_2N$	$C_{22}H_{24}BN$	$C_{22}H_{36}BN$	$C_{22}H_{14}BF_{10}N$	$C_{19}H_{26}BN$	$C_{19}H_{26}BNO$
formula weight	229.94	313.24	325.34	493.15	279.23	295.23
crystal system	orthorhombic	monoclinic	monoclinic	monoclinic	monoclinic	monoclinic
space group	*Pbca*	P2(1)	*P*2(1)/*n*	*P*2(1)/*c*	*P*2(1)/*c*	*P*2(1)/*n*
a (Å)	14.1854(4)	10.1559(5)	8.5311(5)	12.6394(4)	9.6978(5)	8.4770(4)
b (Å)	20.6850(6)	16.5857(8)	17.7333(11)	19.7683(7)	7.7722(4)	18.3487(9)
c (Å)	23.3812(8)	10.8949(6)	13.3028(8)	15.9329(5)	22.4589(13)	11.5037(5)
α (deg)	90.00	90.00	90.00	90.00	90.00	90.00
β (deg)	90.00	106.3827(18)	105.6576	91.9819(20)	93.3801(34)	102.7405(23)
γ (deg)	90.00	90.00	90.00	90.00	90.00	90.00
V (Å^3)	6860.605(538)	1760.665(256)	1937.822(303)	3978.617(297)	1689.863(213)	1745.263(193)
Z	24	4	4	8	4	4
d(calc) g cm^{-1}	1.336	1.182	1.112	1.647	1.097	1.124
abs coeff, *μ*, cm^{-1}	5.3	0.7	0.6	1.6	0.6	0.7
data collected	7868	9266	4014	2874	4254	4244
data $F_o^2 > 3\sigma(F_o^2)$	6291	8168	2901	2119	3028	3053
variables	388	439	220	619	200	264
R	0.0373	0.0460	0.0463	0.0285	0.0688	0.0541
R_w	0.090	0.1169	0.1188	0.0508	0.2102	0.1610
goodness of fit	1.031	1.043	1.034	0.891	1.054	1.055

Fourier map calculation as well as the magnitude of residual electron densities in each case were of no chemical significance. Additional details are provided in the Supporting Information.

Computational Studies. All calculated structures were minimized using the Gaussian 03 program[21] at the B3LYP/6-31 g(d) level of theory. All minimized structures were found to contain no imaginary frequencies, unless otherwise noted. Transition states contained only one imaginary frequency, and the transition states were connected to the minimized structures via IRC analysis, unless otherwise noted.

(21) Frisch, M. J.; Trucks, G. W.; Schlegel, H. B.; Scuseria, G. E.; Robb, M. A.; Cheeseman, J. R.; J. A. Montgomery, J.; Vreven, T.; Kudin, K. N.; Burant, J. C.; Millam, J. M.; Iyengar, S. S.; Tomasi, J.; ; Barone, V.; Mennucci, B.; Cossi, M.; Scalmani, G.; Rega, N.; Petersson, G. A.; Nakatsuji, H.; Hada, M.; Ehara, M.; Toyota, K.; Fukuda, R.; Hasegawa, J.; Ishida, M.; Nakajima, T.; Honda, Y.; Kitao, O.; Nakai, H.; Klene, M.; Li, X.; Knox, J. E.; Hratchian, H. P.; Cross, J. B.; Bakken, V.; Adamo, C.; Jaramillo, J.; Gomperts, R.; Stratmann, R. E.; Yazyev, O.; Austin, A. J.; Cammi, R.; Pomelli, C.; Ochterski, J. W.; Ayala, P. Y.; Morokuma, K.; Voth, G. A.; Salvador, P.; Dannenberg, J. J.; Zakrzewski, V. G.; Dapprich, S.; Daniels, A. D.; Strain, M. C.; Farkas, O.; Malick, D. K.; Rabuck, A. D.; Raghavachari, K.; Foresman, J. B.; Ortiz, J. V.; Cui, Q.; Baboul, A. G.; Clifford, S.; Cioslowski, J.; Stefanov, B. B.; Liu, G.; Liashenko, A.; Piskorz, P.; Komaromi, I.; Martin, R. L.; Fox, D. J.; Keith, T.; Al-Laham, M. A.; Peng, C. Y.; Nanayakkara, A.; Challacombe, M.; Gill, P. M. W.; Johnson, B.; Chen, W.; Wong, M. W.; Gonzalez, C.; Pople, J. A. *Gaussian 03*, Revision E.01; Gaussian, Inc.: Wallingford, CT, 2004.

Results and Discussion

***o*-Benzylphosphino-boranes.** Targeting benzyl linked phosphino-boranes, the species *o*-$BrC_6H_4CH_2PtBu_2$ (**1**) was prepared via simply refluxing an acetone solution of $ClPtBu_2$ with $BrC_6H_4CH_2Br$ for 16 h, followed by a basic aqueous workup. Subsequent vacuum distillation resulted in the isolation of **1** in 52% yield. Lithiation of **1** was readily accomplished with *n*-BuLi in hexanes,[18] and the resulting product $LiC_6H_4CH_2PtBu_2$ (**2**) precipitated from solution, allowing its isolation. Interestingly, lithiations of **1** in coordinating solvents such as Et_2O gave no conversion, inferring the insolubility of **2** in hexanes drives the reaction to completion. The ^{31}P NMR (C_6D_6) of **2** was found to shift minimally from 34.2 ppm for **1** to 32.5 ppm for **2**. Subsequent reaction of **2** with BCl_3 in hexanes gave initially a purple solution which gradually became colorless with a white precipitate. This was attributed to the initial formation of a P−B adduct **2**-BCl_3, which gradually transforms to a thermodynamic product, *o*-$(Cl_2B)C_6H_4CH_2PtBu_2$ **3** (Scheme 1). This product was isolated in 38% yield. Although unconfirmed, the diminished yield was attributed to further reaction of **3** with **2**. The formulation of **3** was supported by the observation of the ^{31}P NMR signal at 31.2 ppm and

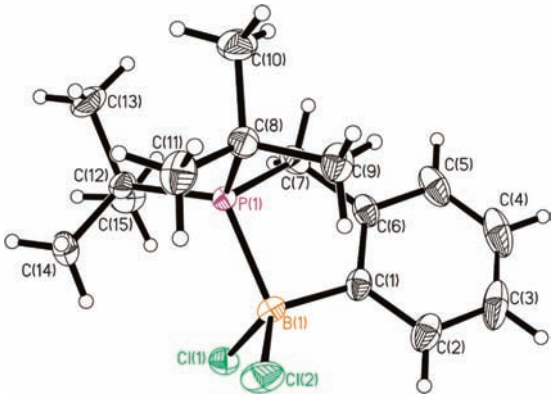

Figure 1. ORTEP drawing of **3**. Thermal ellipsoids are drawn at 50% probability.

Scheme 1. Syntheses of *o*-Benzylphosphino-boranes **3**−**8**

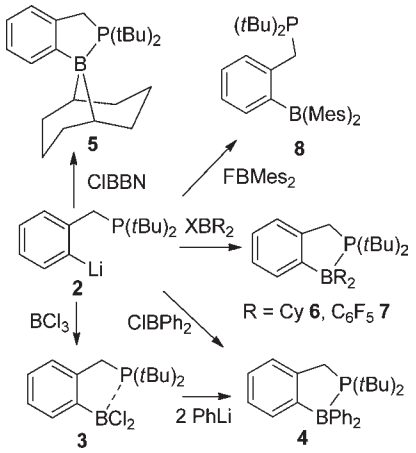

the ^{11}B resonance at 0.02 ppm. The observation of the B−P coupling constant of 96.5 Hz suggested a P−B dative bond. An X-ray crystallographic study (Figure 1) confirmed that the B is coordinated to P with a P−B bond length of 2.024(2) Å. This distance is shorter than that reported for the related benzylic phosphine-borane tBu$_2$BC$_6$H$_4$CH$_2$-PPh$_2$ (2.108 Å)[22] consistent with the greater Lewis acidity and basicity of the B and P centers respectively in **3**.

The lithiated species **2** also reacts with ClBPh$_2$ to give **4** which was isolated in 61% yield. Alternatively, this product can also be synthesized from the addition of 2 equiv of PhLi to **3** affording **4** in 80% yield (Scheme 1). **4** showed similar NMR spectra to **3**, suggesting the presence of a P−B bond. X-ray analysis (Figure 2) confirmed the structure of **4** is similar to that seen for **3** although the P−B bond length (2.064(3) Å) was found to lengthen by 0.04 Å in comparison to **3**. This longer P−B bond is consistent with the lesser Lewis acidity and increased steric bulk about the B-center.

In a similar fashion the species *o*-(BBN)C$_6$H$_4$CH$_2$-PtBu$_2$ (**5**), *o*-(R$_2$B)C$_6$H$_4$CH$_2$PtBu$_2$ (R = Cy **6**, C$_6$F$_5$ **7**, Mes **8**) were synthesized from hexane solutions of their respective chloroboranes, in yields ranging from 61% to 99% (Scheme 1). The ^{1}H, ^{11}B, and ^{31}P NMR of **5** and **6** exhibited similar spectral attributes to those of **3** and **4**. Interestingly, the NMR spectra of **7** are temperature dependent (see Supporting Information). On cooling to −60 °C, the ^{1}H spectrum shows distinct signals for each

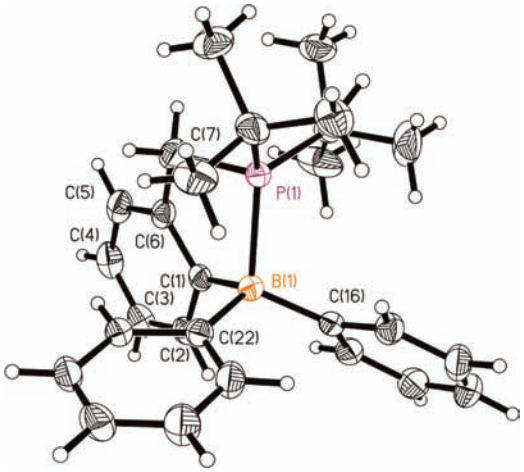

Figure 2. ORTEP drawing of **4**. Thermal ellipsoids are drawn at 50% probability.

of the t-butyl-groups. These signals coalesce at −13 °C and show a single resonance at room temperature. Similar behavior is observed for the benzylic protons, as two distinct signals are seen at −60 °C, where coupling to the phosphorus center is seen. In addition, one of the benzylic protons also exhibits through-space coupling to a fluorine atom (J_{FH} = 13.3 Hz) of a C$_6$F$_5$ group. The ^{19}F-NMR spectrum of **7** shows 10 distinct signals for the fluorine atoms at −60 °C. These signals coalesce to 3 signals at 10 °C. In contrast, the ^{11}B and ^{31}P NMR spectra showed no temperature dependence. These data are consistent with the fluxionality of a five-membered ring resulting from a weak P−B bond. At low temperature the inequivalent C$_6$F$_5$ rings arise from axial and equatorial dispositions together with inhibited rotation about the B−C bonds.

The ^{1}H NMR spectrum of **8** showed sharp peaks in the phenyl region, with broad peaks for both the benzylic and the tBu protons suggesting a less rigid structure. This is reminiscent of 1-*N*-2,2,6,6-tetramethylpiperidine-(CH$_2$)[B(C$_6$F$_5$)$_2$]C$_6$H$_4$.[13,14] The upfield ^{31}P NMR signal and downfield ^{11}B NMR peak for **8** are consistent with three coordinate phosphine and boron centers, suggesting the absence of a dative P−B bond in this case. Crystallographic analyses for **5**−**7** (Figure 3−5) confirmed that the B−P bond lengths of 2.119(2) Å, 2.179(6) and 2.082(3) Å for **5**−**7**, are longer than those in **3** and **4**. In contrast, the structural data for **8** (Figure 6) confirmed the absence of a P−B bond, as the tBu$_2$P and the BMes$_2$ groups were oriented away from each other with a intramolecular P···B separation of 4.910 (5) Å. This is presumably results from the combination of sterically demanding substituents on the P and B centers.

α-Methylbenzyl(*N*,*N*-dimethyl)amine-Boranes. Employing similar synthetic strategies analogous amine-borane systems were targeted. Use of rac-α-methylbenzyl(*N*,*N*-dimethyl)amine as a ligand scaffold provides the additional steric feature of the methyl substituent on the benzylic carbon. Employing metalation of the benzyl-amine PhCH-(Me)NMe$_2$ to generate *o*-LiC$_6$H$_4$CH(Me)NMe$_2$ (**9**), subsequent treatment with BCl$_3$ affords *o*-(Cl$_2$B)C$_6$H$_4$CH(Me)-NMe$_2$ (**10**) (Scheme 2). In a fashion similar to that used to prepare **4**, arylation of **10** with PhLi affords *o*-(Ph$_2$B)C$_6$H$_4$-CH(Me)NMe$_2$ **11**. Alternatively **11** could be prepared from

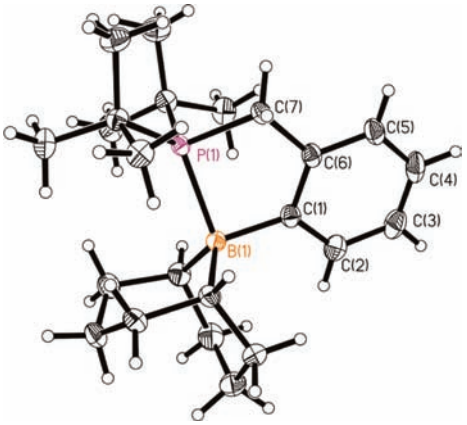

Figure 3. ORTEP drawing of **5**. Thermal ellipsoids are drawn at 50% probability.

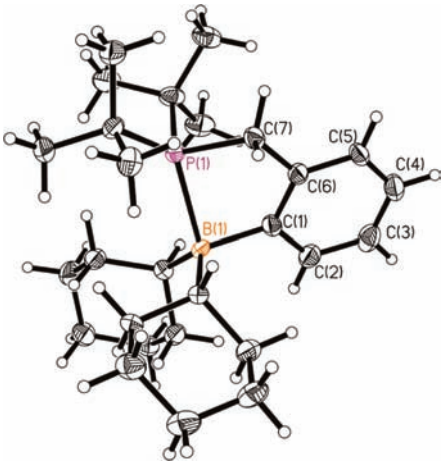

Figure 4. ORTEP drawing of **6**. Thermal ellipsoids are drawn at 50% probability.

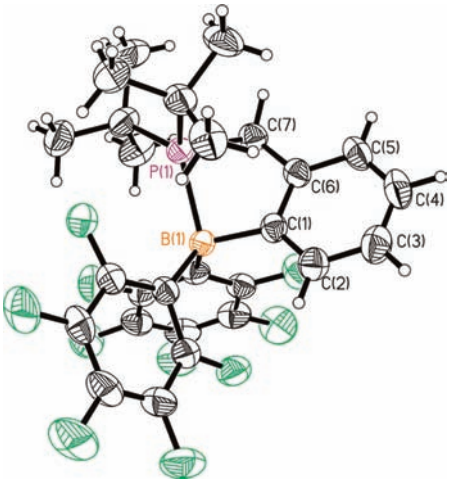

Figure 5. ORTEP drawing of **7**. Thermal ellipsoids are drawn at 50% probability.

the reaction of **9** with $ClBPh_2$. The corresponding species *o*-$(R_2B)C_6H_4CH(Me)NMe_2$ (Cy **12**, C_6F_5 **13**, Mes **14**) were prepared using **9** with the corresponding borane precursors, XBR_2 (Scheme 2). The spectroscopic data for these compounds are consistent with these formulations and similar to

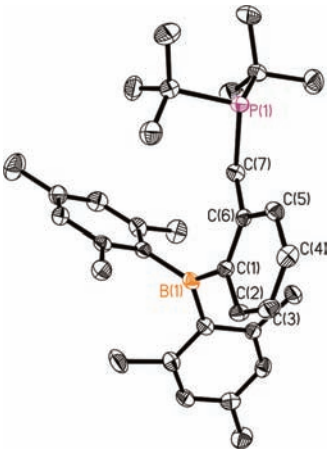

Figure 6. ORTEP drawing of **8**. Thermal ellipsoids are drawn at 50% probability.

Scheme 2. Syntheses of *o*-Phenethyldimethylamino-Boranes **9**−**14**

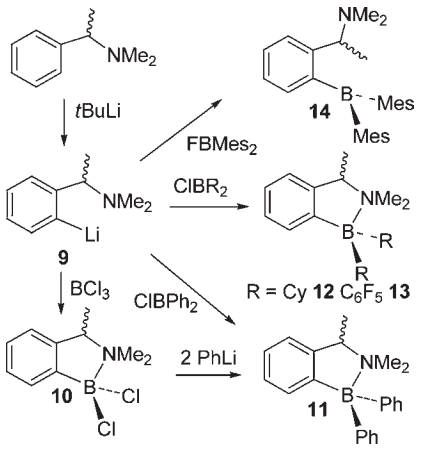

those described for the P-based analogues described above. Crystallographic characterization of **10**−**13** (Figure 7−10) revealed B−N distances of 1.637(2) Å, 1.738(3) Å, 1.754(6) Å, and 1.666(3) Å, respectively, and a benzylic methyl group in the axial position with respect to the five-membered BNC_3 rings. These bond distances reflect both the steric demands and the electronic nature at the B center. In the case of **10** and **13** the electron withdrawing nature of the B-substituents results in comparatively short B−N bonds. The converse is true for the cases of **11** and **12**, where electron donating substituents, lessen the electrophilicity of the B centers.

Toyota and co-workers developed a concept to gauge the strength of a donor−acceptor bonds in benzylic amine-borane complexes[23] known as percent tetrahedral character (%THC). These initial studies examined the deviation of the bond angles around boron from 109.5° to quantify the B−N bond strength.[23,24] Hopfl expanded this approach further to include all of the angles around boron and the donor (Figure 11), using eq 1 to correlate %THC values with adduct strength.[25] This approach was

(22) Mueller, G.; Lachmann, J. *Z. Naturforsch., B: Chem. Sci.* **1993**, *48*, 1248–1256.
(23) Toyota, S.; Oki, M. *Bull. Chem. Soc. Jpn.* **1992**, *65*, 1832–1840.
(24) Toyota, S.; Oki, M. *Bull. Chem. Soc. Jpn.* **1992**, *65*, 2215–2220.
(25) Hopfl, H. *J. Organomet. Chem.* **1999**, *581*, 129–149.

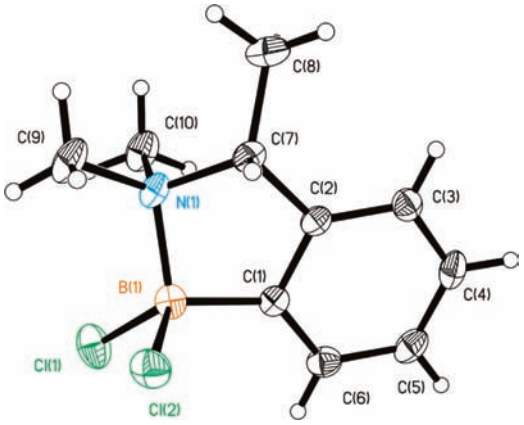

Figure 7. ORTEP drawing of **10**. Thermal ellipsoids are drawn at 50% probability.

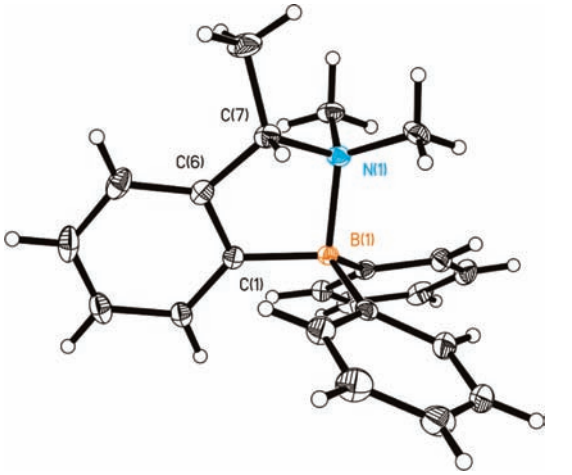

Figure 8. ORTEP drawing of **11**. Thermal ellipsoids are drawn at 50% probability.

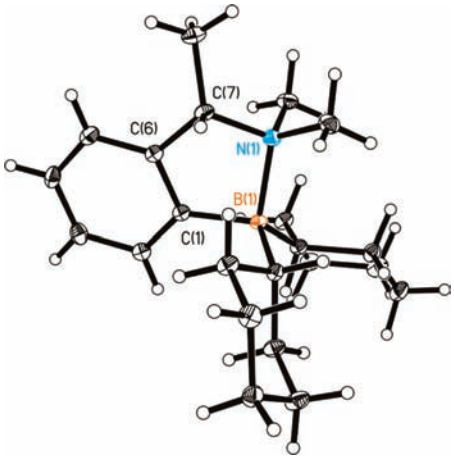

Figure 9. ORTEP drawing of **12**. Thermal ellipsoids are drawn at 50% probability.

applied to the present compounds (Table 2). As expected the two complexes, **3** and **4** with the shortest experimental P−B bond distances resulted in the highest %THC consistent with strong bonds. The P−B bond for **7** was found to have a similar %THC to **6**, despite the experimental observation that the former species exhibits a somewhat

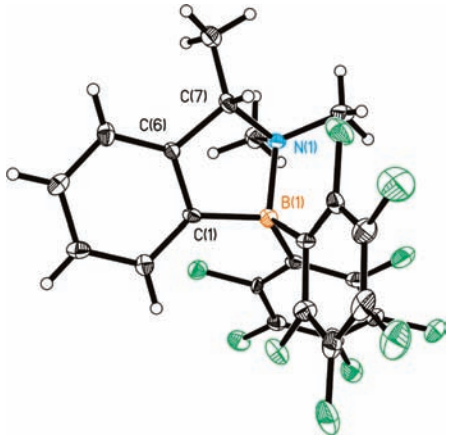

Figure 10. ORTEP drawing of **13**. Thermal ellipsoids are drawn at 50% probability.

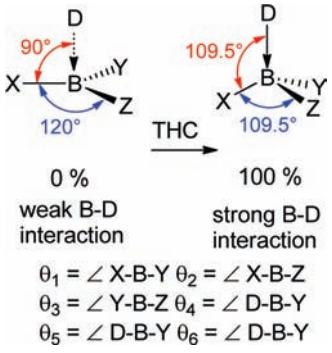

Figure 11. Percent tetrahedral character (THC) of a Lewis acid−base adduct.

shorter B−P distance In the same vein, the B−P bond in **5** is significantly shorter than in **6** and yet the %THC is higher in the latter species. Calculations for the one previously reported analogue, tBu$_2$BC$_6$H$_4$CH$_2$PPh$_2$ gave a %THC of 61.2%,[22] while the related 5-member rings species R$_2$PC$_3$H$_6$B(C$_6$F$_5$)$_2$ (R = Ph, tBu) gave %THCs of 57.8 and 70.8%, respectively).[26] Collectively these data demonstrated the impact of steric demands on B−P bond lengths and the pyramidalization of B, although the % THC does not strictly correlate with bond distance in these systems.

$$\%\mathrm{THC} = \left[1 - \frac{\sum_{n=1-6} |109.5 - \theta_n|^\circ}{90^\circ}\right] \times 100 \qquad (1)$$

Calculation of the %THC from these structural data reveals that **10**−**13** exhibits consistently greater pyramidalization of B compared to the P-analogues **3**, **4**, **6** and **7**. This observation presumably relates to the presence of the sterically less encumbered donor, in the amino-borane derivatives.

Reactivity of Benzylic Phosphino- and Amino-borane Complexes. Efforts to affect the catalytic hydrogenation of tBuN=CHPh at 100 °C for several days employing 5 mol % of **3**, **4**, **5**, and **6** under a H$_2$ atmosphere were

(26) Spies, P.; Froehlich, R.; Kehr, G.; Erker, G.; Grimme, S. *Chem.—Eur. J.* **2008**, *14*, 333–343.

Table 2. Experimental and Theoretical Bond Distances and %THC

	experimental		theoretical	
complex	P(N)−B distance (Å)	%THC	P(N)−B distance (Å)	%THC
3	2.024(2)	72.0	2.057	73.2
4	2.064(3)	63.7	2.196	59.8
5	2.119(2)	47.6	2.321	49.8
6	2.179(6)	54.3	2.451	45.7
7	2.082(3)	54.7	2.146	50.8
10	1.637(2)	79.5	1.696	66.0
11	1.738(3)	68.1	1.826	61.4
12	1.754(6)	67.7	1.829	65.7
13	1.666(3)	60.7	1.724	56.3

Scheme 3. Syntheses of **15** and **16**

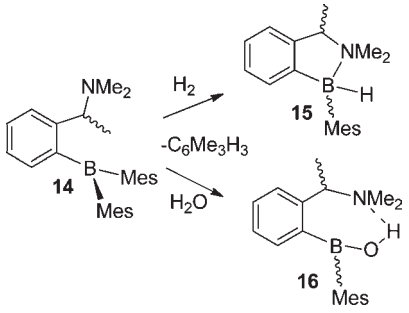

unsuccessful. There are a number of possible explanations for this observation. In contrast to other catalytically active phosphino-borane species, it could be that the P−B bond in the present species is strong and fails to open to permit the heterolytic activation of H_2. Alternatively it could be that inclusion of B centers in **3**−**6** are insufficiently Lewis acidic to stabilize the H_2 adduct resulting in rapid elimination of H_2 reforming the P−B bond. In marked contrast, **7** and **8** were found to react with H_2 at elevated temperatures (100 °C). In these cases, elimination of HC_6F_5 and mesitylene were evident from the characteristic ^{1}H and ^{19}F NMR signals; however, the nature of resulting B−P products could not be unambiguously confirmed as all efforts to isolate these products were unsuccessful. Treatment of **14** with H_2 gave no reaction at ambient conditions, but increasing the temperature to 100 °C resulted in the formation of two new diastereomeric complexes in a ratio of 3: 2. Crystallographic analysis confirmed the presence of chiral C and B centers and thus identified the (*S*,*S*) isomer of *o*-((Mes)HB)C_6H_4CH(Me)NMe_2 **15** (Scheme 3, Figure 12), in which the α-methyl group adopts an axial position in the 5-membered chelate ring that results from coordination of N to B. The B−N bond length was determined to be 1.674(3) Å. Interestingly dissolution of the crystals of **15** gave rise to a diastereomeric mixture identical to that obtained from the initial reaction mixture of **14** + H_2. This suggests that epimerization of the chiral B center is facile. In a similar vein, although **14** was stable in dry air, exposure to small amounts of water over the course of days at room temperature resulted in the slow conversion of **14** to the species *o*-((Mes)HOB)C_6H_4CH(Me)NMe_2 **16** with the loss of mesitylene. Spectroscopic and crystallographic data were consistent with the formulation of **16** (Scheme 3, Figure 13). Strong hydrogen bonding between the ammonium center and the boronic acid fragment is evident as

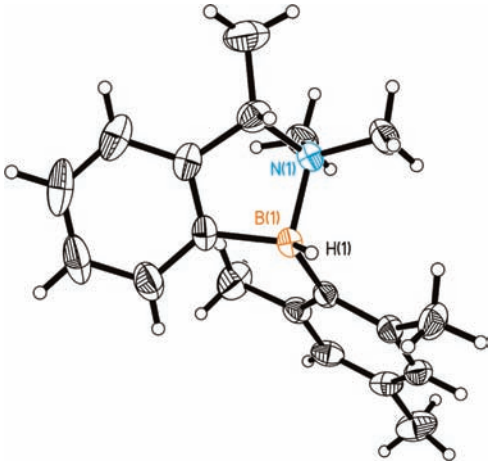

Figure 12. ORTEP drawing of **15**. Thermal ellipsoids are drawn at 50% probability.

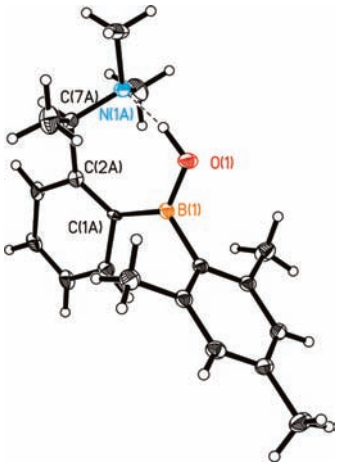

Figure 13. ORTEP drawing of **16**. Thermal ellipsoids are drawn at 50% probability.

the B−O and N−H distances were found to be 1.335(2) Å and 1.589(3) Å, respectively.

Computational Studies. To garner further insight into the structure−reactivity relationship, the present phosphino-boranes **3**−**8** and amino-boranes **10**−**14** were examined computationally using the Gaussian 03 program at the B3LYP/6-31 g(d) level of theory (Table 2).[21] Previous literature infers that the limitations of the B3LYP/6-31G* approach particularly in the computation of interaction energies for donor−acceptor adducts can give rise to large errors as these functionals do not properly account for medium-range correlation effects.[27−30] However these conclusions continue to be the subject of controversy.[31] Nonetheless, the minimized structures were found to be very similar to those observed experimentally. The largest deviation between experimental and theoretical B−P(N) distances, of about 0.2 Å, was observed in the structures **5** and **6**. A similar observation was

(27) Grimme, S. *Angew. Chem., Int. Ed.* **2006**, *45*, 4460.
(28) Plumley, J. A.; Evanseck, J. D. *J. Phys. Chem.* **2007**, *111*, 13472.
(29) Schwabe, T.; Grimme, S. *Acc. Chem. Res.* **2008**, *41*, 569.
(30) Rakow, J. R.; Tüllmann, S.; Holthausen, M. C. *J. Phys. Chem. A.* **2009**, *113*, 12035.
(31) Simon, L.; Goodman, J. M., *Org. Biomol. Chem.* **2010**, DOI: 10.1039/c0ob00477d.

Table 3. Calculated ΔG Energies for the Reaction H_2 with *o*-Benzylphosphinoboranes

precursor	$\Delta G^{\ddagger}$ (H_2) (kcal/mol)	*o*-(R_2BH)C_6H_4CH(Me)$NHMe_2$ (kcal/mol)
3	38.0	21.1
4	32.1	21.0
5	28.3	26.3
6	28.3	25.7
7	31.6	13.2
8	no t.s. found	31.7

Table 4. Calculated ΔG Energies for the Reaction H_2 with *o*-Methylbenzylaminoboranes

precursor	$\Delta G^{\ddagger}$ (H_2) (kcal/mol)	*o*-(R_2BH)C_6H_4CH(Me)$PHtBu_2$) (kcal/mol)
10	43.8	25.6
11	30.6	24.2
12	24.3	21.2
13	30.4	14.3
14	24.3	19.5

Scheme 4. Reaction Coordinate Diagram for the Reaction of H_2 with **7**

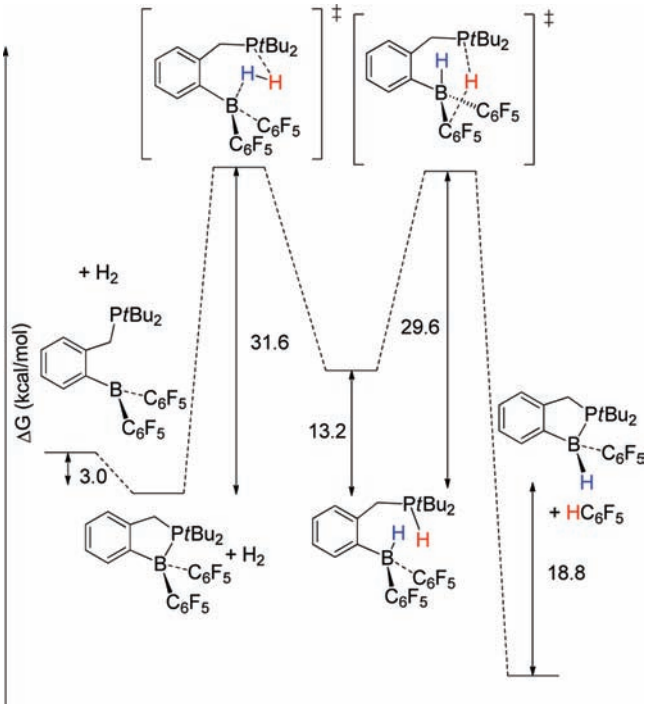

made by Gilbert in his theoretical analysis of B−N bonds.[32] The reactivity of these species with H_2 was also probed computationally (Table 3 and Table 4). The computed energies for the products of hydrogenation, the phosphonium hydridoborates, were found to be similar for the products from **5** and **6** while those derived from **3** and **4** were slightly lower in energy. However, in all cases these products were endothermic with respect to the precursor phosphine-boranes and H_2. The barriers to H_2 activation were also computed and found to be in the range of 28−38 kcal/mol, although a transition state was not found for **8**. In these cases, the high barrier and endergonic nature of the products are in accord with the

(32) Gilbert, T. M. *J. Phys. Chem.* **2004**, *108*, 2550–2554.

Scheme 5. Reaction Coordinate Diagram for the Reaction of H_2 with **14**

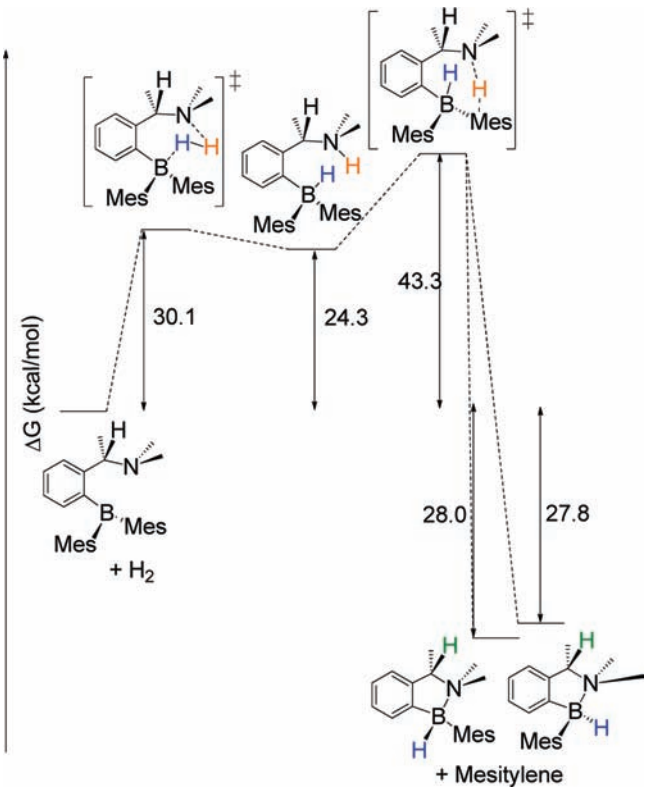

experimental observation that these species do not react with H_2.

In the case of the reaction of **7** with H_2, calculations show a small stabilization of 3.0 kcal/mol is achieved by the formation of the dative P−B bond. This is consistent with the experimental observation of an equilibrium between an open and closed forms in solution. The activation energy for the reaction with H_2 is computed to be 31.6 kcal/mol (Scheme 4). Subsequent heterolytic cleavage to generate a phosphonium borate results as the product is 20 kcal/mol lower in energy (ΔG) than the transition state, but endergonic by 13.2 kcal/mol with regards to **7** and H_2. From this salt the activation barrier for proton transfer to a B-bound C_6F_5 group is 2 kcal/mol less than that for the elimination of H_2. Thus, loss of HC_6F_5 proceeds resulting in the formation of *o*-(C_6F_5BH)$C_6H_4CH_2PtBu_2$ which is exergonic (ΔG) by almost 19 kcal/mol in comparison to **7** and H_2 (Scheme 3). The loss of HC_6F_5 is thought to be entropy driven as the loss of HC_6F_5 relieves much of the steric congestion allowing formation of a stronger dative P−B bond in *o*-(C_6F_5BH)$C_6H_4CH_2PtBu_2$. This computed reaction coordinate is consistent with the experimental observations that the reaction of **7** with H_2 proceeds at elevated temperatures to give HC_6F_5, although the P/B species could not be isolated. The formation of the dative bond in *o*-(C_6F_5BH)$C_6H_4CH_2PtBu_2$ precludes further reaction with H_2. A similar reaction is expected for **8** although the loss of a mesitylene from the reaction of **8** and H_2 was not probed computationally.

Similar calculations for the reaction of **14** with H_2 (Scheme 5) revealed a similar reaction path as observed for **7**. In the case of the amino-borane species, the $\Delta G^{\ddagger}$

associated with the activation barrier to the heterolytic activation of H_2 was computed to be 30.1 kcal/mol, similar to that seen for the phosphino-borane above. However, the subsequent loss of mesitylene and generation of **15** was much more exergonic, as **15** was computed to be 28.0 kcal/mol (ΔG) lower in energy than **14**. The driving force for this proton transfer is that the loss of mesitylene. The resulting homochiral **15** was found to be 0.3 kcal/mol lower in energy than its diastereomer, which is in accord with the experimentally observed 3:2 ratio of the diastereomers. The low activation barrier of epimerization of the chiral B center of 14.8 kcal/mol is consistent with observed rapid equilibration of the two diastereomers.

Conclusions

A series of linked phosphine and amine-boranes species have been prepared and studied. Introduction of a dialkyl or diaryl boron centers resulted in species that give rise to intramolecular B−P or B−N dative bonds. Groups such as C_6F_5 and mesityl substituents on B result in weaker or no dative bonds. Reaction of these latter species with H_2 are shown to exhibit accessible activation barriers, resulting in the activation of heterolytic cleavage of H_2 and subsequent loss of an aryl substituent from B and the formation of new five-membered B−P ring derivatives.

These data, demonstrate that sterically demanding donor fragments are essential for H_2 activation. However, proximity of the base and acid sites can favor donor−acceptor adduct formation as well as prompt substituent elimination reactions. This latter issue can be potentially avoided with judicious modification of the basicity of the Lewis base. However, the design of new bifunctional metal-free hydrogenation catalysts must also account for the ability of the Lewis basic site to deliver a proton to the substrate during hydrogenation catalysis. The study of the structure−reactivity relationships and the design of new FLP hydrogenation catalysts continue to be a subject of intense efforts in our laboratories.

Acknowledgment. The authors thank NSERC of Canada for financial support. D.W.S. is grateful for the award of a Canada Research Chair and a Killam Research Fellowship. This research was supported by NSERC. Z.M.H. is grateful for the award of an Ontario Postdoctoral Fellowship.

Supporting Information Available: Crystallographic data in CIF format, 3D coordinates and energies of all calculated structures, variable temperature NMR of **7** and **14**. This material is available free of charge via the Internet at http://pubs.acs.org.